Site-Directed Fluorescence Studies of a Prokaryotic ClC Antiporter†

Susan P. Bell,‡ Patricia K. Curran, Sean Choi,§ and Joseph A. Mindell*

Membrane Transport Biophysics Unit, Porter Neuroscience Center, National Institute of Neurological Disorders and Stroke, National Institutes of Health, Bethesda, Maryland 20892

Received November 21, 2005; Revised Manuscript Received April 6, 2006

ABSTRACT: Channels and transporters of the ClC family serve a variety of physiological functions. Understanding of their gating and transport mechanisms remains incomplete, with disagreement over the extent of protein conformational change involved. Using site-directed fluorescence labeling, we probe ClC-ec1, a prokaryotic ClC, for transport-related structural rearrangements. We specifically label cysteines introduced at several positions in the R helix of ClC-ec1 with AlexaFluor 488, an environment-sensitive fluorophore, and demonstrate that the labeled mutants show H^+/Cl^- transport activity indistinguishable from that of the wild-type protein. At each position that we examined we observe fluorescence changes upon acidification over the same pH range that is known to activate transport. The fluorescence change is also sensitive to Cl^- concentration; furthermore, the Cl^- and H^+ dependencies are coupled as would be expected if the fluorescence change reflected a conformational change required for transport. Together, the results suggest that the changes in fluorescence report protein conformational changes underlying the transport process. Labeled transporters mutated to remove a glutamate critical to proton-coupled chloride transport retain pH-dependent fluorescence changes, suggesting that multiple residues confer pH dependence on the transport mechanism. These results have implications for models of transport and gating in ClC channels and transporters.

The ClCs represent a broad and functionally polymorphic family of anion transport proteins. ClC genes abound in all kingdoms; in mammals, these proteins perform a variety of physiological functions, from maintaining the resting membrane potential in muscle to mediating transepithelial Cl^- secretion in kidney (*1*). Understanding of these proteins has advanced rapidly in recent years, with the determination of X-ray crystal structures of two prokaryotic ClCs (*2*) as well as the elucidation of functional roles for many of these proteins using genetic approaches (*3*). Most surprising was the recent revelation that the *Escherichia coli* ClC is not a chloride channel but, rather, functions as a H^+/Cl^- antiporter (*4*). Despite this progress, our understanding of the physical processes underlying ClC function remains sketchy and incomplete.

Gating in ClC proteins is complex and incompletely understood. The ClCs are homodimeric proteins with two distinct transport pathways, one in each subunit. The best-studied ClC channels, ClC-0 and ClC-1, display two distinct gating processes, a "fast" gate which gates the two pores independently and a "slow" gate that closes both pores simultaneously. Recently, Dutzler and MacKinnon proposed a model for the fast gate based on X-ray crystal structures of prokaryotic ClCs (*5*). In the original structures, a glutamate residue (position 148 in ClC-ec1, in contact with the extracellular aqueous compartment) occludes the presumed chloride permeation pathway. In contrast, the structure of a mutant in which glutamate 148 is replaced with glutamine reveals that residue's side chain has moved away from the pore and has been replaced with a chloride ion. On the basis of these observations, the authors proposed that the movements of this glutamate in and out of the permeation pathway account for the fast gating behavior of ClC channels. Indeed, experiments in that paper, as well as in subsequent publications (*5*−*7*), demonstrate that mutations at that position have a strong influence on the pH dependence and rectification properties of eukaryotic ClCs. Data from other experimental approaches, however, argue that the fast gate may be more complicated than the movement of a single glutamate. Hints come from the state dependence of block by cytoplasmic agents (*8*, *9*), as well as the limited effects on ClC-0 channel properties of mutating a conserved, Cl^--coordinating residue (Tyr512 in ClC-0 corresponding to Tyr445 in ClC-ec1) (*10*).

Thus, the structural model proposed for the ClC fast gate cannot account for all of the functional observations. Do these differences result from differences in mechanism between ClC channels and transporters? Or is the "gating glutamate" a component of a more complex gating machinery in all of the ClCs? If so, what other protein rearrangements are required for ClC gating? Neither the protein movements comprising any conformational changes aside from the gating

† This work was supported by the Intramural Program of the National Institute of Neurological Disorders and Stroke, National Institutes of Health.

* To whom correspondence should be addressed: MTBU, NINDS, NIH, 35 Convent Dr., Bldg. 35, MSC 3701, Bethesda, MD 20892. Phone: (301) 402-3473. Fax: (301) 480-1693. E-mail: mindellj@ninds.nih.gov.

‡ Current address: Department of Medicine, Johns Hopkins University, Baltimore, MD 21287.

§ Current address: Department of Biomedical Engineering, Johns Hopkins University, Baltimore, MD 21287.

10.1021/bi0523815
Published on Web 05/10/2006

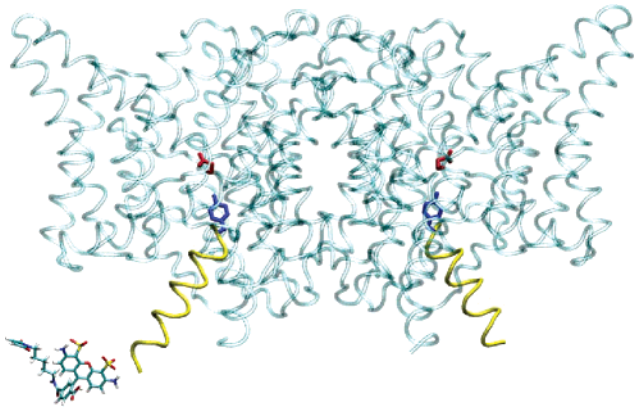

FIGURE 1: Structure of ClC-ec1. The protein backbone from Protein Data Bank entry 1OTS is viewed parallel to the membrane plane in cyan, with the R helix highlighted in yellow (Fab fragments are not shown). The side chain of glutamate 148 is colored red, and that of tyrosine 445 is colored blue. At the bottom, an energy-minimized structure of Alexa488 maleimide is shown drawn to scale for size comparison. The cyan portion of the protein backbone is semitransparent to facilitate visualization of internal structures. Structures were viewed in VMD (*23*, *24*) and rendered in POVray (www.povray.org); the fluorophore was drawn and energy-minimized in ChemDraw (CambridgeSoft) and viewed in VMD.

glutamate nor their presence or absence in a prokaryotic ClC has been examined.

We have begun to address these questions by applying site-directed fluorescence experiments to a prokaryotic ClC. We sought to determine whether regions of the protein beyond glutamate 148 are moving during transport. These experiments involve introducing a cysteine at a given location in the protein, covalently coupling a fluorescent probe, and monitoring changes in fluorescence under conditions that activate the transport process. The fluorophore we used, AlexaFluor 488, is sensitive to its local solvent environment (*11*) and has been used to detect protein conformational changes (*12*). If the protein undergoes a conformational change upon transporting ions, we might therefore expect to find one or more positions where the fluorescence depends on the activation state of the transporter. This approach has been used successfully to monitor conformational changes in other membrane proteins, including the β-adrenergic receptor (*13*) and potassium channels (*14*−*16*), among others.

For these experiments, we labeled residues on or near the R helix of ClC-ec1 (Figure 1, yellow helix); this unusually positioned α helix begins deep in the presumably membrane-embedded portion of the protein and extends into the cytoplasmic aqueous compartment. The R helix has been proposed as a possible site of transporter regulation by intracellular processes (*2*) because Tyr445, on its N-terminal end, is involved in coordinating a permeant ion even as the helix extends into the intracellular compartment. One face of helix R lines the inner vestibule of the presumed Cl^- transport pathway, and tyrosine 445 also at least partially occludes access to the central Cl^--binding site. We reasoned that since the R helix bridges the protein core and the cytoplasm, even a small conformational change might move at least one residue across the protein−water boundary and cause a detectable change in fluorescence. Indeed, we find that fluorescent labels attached at multiple positions in helix R demonstrate fluorescence changes upon acidification, suggesting that this helix or nearby parts of the protein undergo a conformational change. Our results suggest that conformational changes in ClC-ec1 extend beyond glutamate 148 and propagate to the intracellular side of the protein. Furthermore, we find evidence that the conformational change could involve unexpected parts of the protein. The pH dependence of the change, though coupled to the gating glutamate, may also reflect the titration of other residues.

EXPERIMENTAL PROCEDURES

Chemicals. E. coli polar lipid extract was purchased from Avanti Polar Lipids. *n*-Decyl D-maltopyranoside was purchased from Anatrace. x3-[(3-Cholamidopropyl)dimethylammonio]-1-propanesulfonate was purchased from Pierce Chemical. Endopeptidase LysC was obtained from Roche Chemicals. AlexaFluor 488 C_5-maleimide (Alexa488)[1] was from Invitrogen. Other chemicals were purchased from Sigma Chemical.

Recombinant DNA, Cell Growth, and Protein Purification. The pASK-derived plasmid containing ClC-ec1 with a C-terminal LysC site and His tag was obtained from A. Accardi (*7*). Mutations were generated using standard PCR-based methods; inserts were sequenced in their entirety to verify the presence of the desired mutation and the absence of others. Cultures of freshly transformed BL21(DE3) cells were grown in Terrific Broth to mid-log phase (A_{600} = 1.0) at 37 °C and then induced with anhydrotetracycline at 22 °C for 16 h. Cells were spun, resuspended in 50 mM Tris, 100 mM NaCl, and 5 mM βME (pH 7.5), and disrupted by sonication. Membrane proteins were extracted with 50 mM DM for 2 h. His tag purification was performed on a cobalt affinity column, eluting with 500 mM imidazole. After concentration (Millipore UltraFree) and LysC proteolysis (to remove the His tag), the protein was run on a Superdex 200 10/300 GL column in 10 mM Tris, 150 mM NaCl, 5 mM tris(2-carboxyethyl)phosphine hydrochloride, and 10 mM DM (pH 7.5). Peak fractions were collected and used for labeling with the fluorophore. Assays for free thiol used a kit based on the reduction of cysteamine (Molecular Probes).

Labeling. Alexa488 was dissolved in water, aliquoted, dried in a speed-vac, and stored at −20 °C for future use. Sephadex G-50 (Amersham) was swelled overnight in an excess of flux buffer [10 mM HEPES (pH 7.5), 50 mM NaCl, and 2 mM $CaCl_2$] containing 10 mM DM. The purified protein concentration was determined by the absorbance at OD_{280} using a calculated extinction coefficient. Protein and all tubes were degassed for 1 h and then placed under nitrogen. A 10-fold molar excess of Alexa488 was added to protein and the mixture incubated for 2 h at room temperature. Excess unreacted label was removed on a desalting column. Polystyrene columns (Pierce) filled with swelled Sephadex G-50 were centrifuged to remove excess buffer, loaded with labeled protein, and centrifuged again to separate unbound Alexa488. The protein concentration and labeling efficiency were determined by absorption spectroscopy.

Reconstitution into Liposomes. E. coli polar lipids, dried under N_2 and washed with pentane, were suspended by sonication to a final concentration of 10 mg/mL in flux buffer

[1] Abbreviations: DM, *n*-decyl β-D-maltopyranoside; CHAPS, x3-[(3-cholamidopropyl)dimethylammonio]-1-propanesulfonate; βME, 2-mercaptoethanol; Alexa488, AlexaFluor 488 C_5-maleimide; CCCP, carbonyl cyanide *m*-chlorophenyl hydrazone.

containing 35 mM CHAPS; 100 μg of labeled protein was incubated with 10 mg of lipids for 30 min at room temperature and then the mixture dialyzed overnight to remove the detergent. Samples, frozen in a dry ice/ethanol bath and thawed for three cycles, were then extruded with a miniextruder (Avanti Polar Lipids) for 13 passes through 100 nm membranes and used immediately.

Flux assay reconstitutions were similar except that the initial buffer was 350 mM KCl, 50 mM citric acid, 20 mM sodium phosphate, and 35 mM CHAPS (pH 7.0); the protein-to-lipid ratio was 5 μg of protein/mg of lipid. After dialysis and freezing and thawing, the mixture was acidified to pH 4.5 with phosphoric acid and sonicated; the outside solution was then changed by spinning the sample through a Sephadex G-50 column equilibrated with 300 mM potassium sulfate, 3 mM KCl, and 2 mM L-glutamic acid (pH 4.8) (LC buffer). The choice of detergent for the lipid solubilization is critical; reconstitution using DM-solubilized lipids produces uselessly leaky vesicles.

Fluorescence Measurement. Fluorescence measurements were performed on a Fluoromax-3 (Jobin Yvon) fluorescence spectrophotometer, equipped with Peltier temperature control and polarizers. For experiments with liposomes, dilutions were in FB in the presence of 5 μM carbonyl cyanide *m*-chlorophenyl hydrazone (CCCP). The pH was lowered by adding 1 M citric acid (final concentration of up to 5 mM) and increased with 1 M Tris (pH 9) (final concentration of up to 10 mM). Solubilized, labeled protein was diluted in FB and 10 mM anagrade DM. For anion experiments, the concentrated anions and protein were diluted in low-salt FB [8 mM NaCl, 1 mM $CaCl_2$, and 10 mM HEPES (pH 7.5)]. For all experiments, the excitation wavelength was 493 nm; fluorescence was recorded in a 10 mm quartz cell at 22 °C. All additions were followed by thorough mixing. For free probe experiments (Figure 2), probe concentrations were 0.5−2 μM. Final protein concentrations were 2−5 and 15−25 nM for the detergent-solublized protein and liposome-reconstituted protein, respectively. For each condition, three spectra were acquired and averaged. Data from independent experiments were further averaged for presentation. Data were corrected for volume changes; these never exceeded 5% and never altered the qualitative result.

Flux Experiment for Movement of Protons Driven by a Chloride Gradient. Flux experiments were performed essentially as described in ref *7*. Liposomes containing 350 mM KCl, 50 mM citrate, and 20 mM phosphate (pH 7.0) in LC buffer were added to 2 mL of LC buffer in a tube, and the pH was monitored using a pH electrode (Corning) and recorded on a chart recorder. Transport was initiated with the addition of 1 μg/mL valinomycin. The experiment was terminated by collapsing the proton gradient with the addition of 0.25 μg/mL CCCP or carbonyl cyanide *p*-(trifluoromethoxy)phenylhydrazone. Chart records were scanned and processed using Adobe Photoshop to remove the background grid and enhance the contrast of the recorded trace.

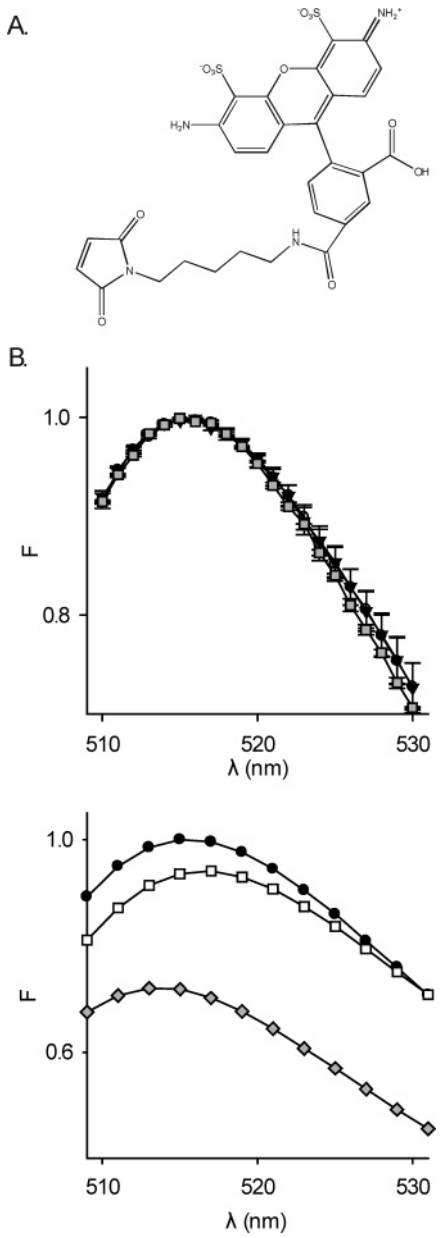

FIGURE 2: Properties of the fluorophore. The structure of Alexa488 is shown in panel A. Emission spectra of the free probe were measured at a series of pH's. (B) Fluorophore emission spectra were measured at pH 7.5 (white circles); subsequently, the cuvette pH was lowered to 4.2 with citric acid (black triangles) and then increased to pH ~7.5 with the addition of Tris (gray squares). Each experiment was normalized to an initial peak emission of 1.0 at pH 7.5. Averaged data from three separate experiments at each pH are shown, with error bars indicating the standard error of the mean. In panel C, emission spectra are shown for equal concentrations of Alexa488 in different solvents. Single spectra are shown for each solvent, including water (black circles), methanol (white squares), and ethanol (gray diamonds) in order of decreasing polarity. The aqueous spectrum was measured in flux buffer (see the text). Spectra were normalized to the aqueous maximum. F represents the normalized fluorescence emission in this and subsequent figures.

RESULTS

Specific Labeling of Mutant Proteins. We sought evidence of conformational changes in the prokaryotic ClC formerly known as EriC, now called ClC-ec1. This protein is readily expressed and purified, and the majority of published structural and functional analyses utilize this protein. We used a construct (kindly provided by A. Accardi) similar to that in ref *17* but with a C-terminal histidine tag instead of the original N-terminal tag. Proteins with R helix mutations generally expressed well, in the range of 0.5−1.5 mg/L of culture. Proteins were purified using a protocol based on the

method of ref *2*, with an initial Co^{2+} chelating column followed by tag cleavage (with lysC protease) and gel filtration. The solutions in our protocol were modified slightly from those published previously; introduced cysteines were kept reduced with βME added in early steps and replaced with tris(2-carboxyethyl)phosphine hydrochloride during gel filtration. This protocol yields a single protein band on an overloaded Coomassie-stained gel (data not shown). All of the mutant proteins reported here gave symmetric peaks on the gel filtration column and eluted in the fractions expected for dimeric ClC-ec1 (data not shown). Since we are not using these proteins for electrophysiology, no attempts to remove trace contaminating porins have been made (*7*).

Our approach is to label the protein with a fluorescent probe and to manipulate the solution conditions (buffer pH and ion concentrations) in ways that are known to affect transport activity and thus might affect the protein conformation. If the protein undergoes a conformational change that alters the local environment of the fluorophore, we would expect to see changes in the fluorescence emission. To be useful in these experiments, a fluorophore's emission properties must (1) depend on the local solvent (i.e., dielectric) environment and (2) be independent of pH and ionic strength in the ranges of interest. We performed controls to test these properties using fluorophores that had been pre-reacted with βME, to approximate the protein-conjugated state. Figure 2 presents the results of these controls for Alexa488, the reagent we used for all experiments presented here. For Alexa488 (chemical structure shown in Figure 2A), both the λ_{max} and the quantum yield depend on the nature of the solvent. The emission intensity depends monotonically on the polarity of the solvent and will be used below as a measure of fluorophore environment. In contrast, the λ_{max} shifts to a slightly longer wavelength between water [Figure 2C (black circles)] and methanol (white squares) and then back toward shorter wavelengths in the more hydrophobic ethanol (gray diamonds). This observation suggests that the λ_{max} will not be useful in attempts to interpret fluorescence changes. Experiments shown in Figure 2B, which shows spectra for the free probe at pH 7.5 (white circles) and 4.2 (black triangles) and once the pH has been restored to 7.5 (gray squares) in a single experiment, also demonstrate that the probe's emission is independent of pH between 7 and 4.2. Results demonstrating that the free probe is also essentially independent of Cl^- concentration in the range of interest are shown in Figure 7D to allow comparison with the relevant experiments.

The wild-type ClC-ec1 protein contains three cysteine residues. Given that simultaneously mutating all three of these residues results in low expression yields (M. Maduke, personal communication), we evaluated the feasibility of using the native protein as a target for cysteine mutagenesis. On the basis of their locations in the structure, the native cysteines are not expected to be accessible from aqueous solution: one of them is exposed to the hydrophobic core of the membrane, and two are buried in the protein core. Thiol assays on the detergent-solubilized wild-type protein revealed no accessible SH groups per protein monomer (not shown). In contrast, similar assays on the single-cysteine mutant, L449C, quantified a single accessible cysteine per monomer (not shown), further suggesting that the native cysteines are inaccessible to aqueous reagents. In addition,

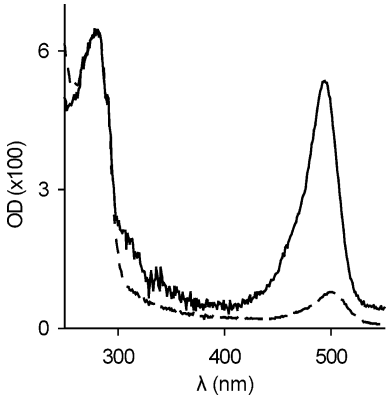

FIGURE 3: Specific labeling of introduced cysteines. Wild-type (WT) and I448C proteins were exposed to equal concentrations of Alexa488 maleimide for 2 h and then spun through an ~3 mL Sephadex G-50 column to remove unreacted probe. Absorption spectra are shown for the column eluates with WT represented by the dashed line and I448C by the solid line. Spectra were normalized to an A_{280} of 1.0. The mutant protein spectrum has a strong absorbance maximum at ~490 nm, which represents covalently attached Alexa488, whereas the WT has a minimal 490 nm peak. The minimal fluorophore peak for the WT sample demonstrates that the three native cysteines are essentially inaccessible to the reagent and that the G-50 column is sufficient for removal of the bulk of the unreacted fluorophore.

the water-soluble fluorescent probe, Alexa488, reacts strongly with the L449C mutant but minimally with the wild-type protein to form a covalent adduct as shown in Figure 3. This figure shows absorbance spectra of wild-type (dashed line) and L449C (solid line) proteins after reaction with a 10-fold molar excess of Alexa488 for 2 h and removal of the excess unreacted fluorophore. The low absorbance of the wild-type protein around 500 nm, the absorption peak of the fluorophore, demonstrates that the native protein is poorly labeled and that our spin column efficiently removes the excess unreacted probe. The fluorophore absorbs light primarily in the visible spectrum, allowing us to use its known extinction coefficient together with that of the protein to determine the extent of labeling for a given preparation. For most constructs, we routinely obtain labeling efficiencies of 85−95%. In general, proteins labeled at >40% are usable in fluorescence measurements in liposomes; at lower levels, it can be difficult to separate the fluorescence emission from scattered light, even with the use of polarizers.

Activity Measurements on Labeled Proteins. We measured the transport activity of each labeled mutant to confirm that the presence of the fluorescent probe does not prevent functional transport. The chloride-driven proton uptake assay is a stringent assay for a properly functioning protein; we use the method described by Accardi and Miller (*4*). We create a large, outwardly directed Cl^- gradient (350 meq/L inside, 3 meq/L outside) across the membranes of proteoliposomes containing reconstituted, labeled ClC-ec1 mutants. In the presence of functional transporters, this gradient will drive protons into the vesicles against their concentration gradient. The outside solution is minimally buffered, so small pH changes are easily measured with a standard pH electrode and documented on a chart recorder. These assays are shown for the wild-type protein and the mutants in Figure 4. Note that since the transporter is electrogenic, we initially observe no proton flux upon addition of vesicles to the cuvette. Only after valinomycin is added to shunt the electrical potential

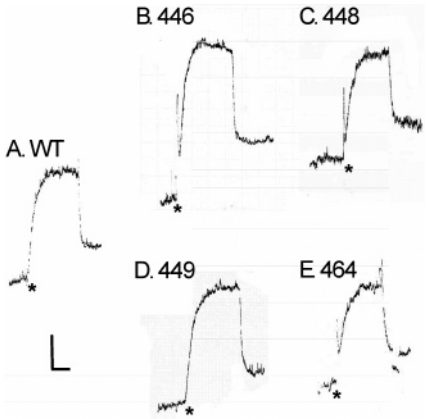

FIGURE 4: Activity measurements of wild-type and labeled mutant proteins. Cl^--driven H^+ uptake was assessed for WT (A) or a mutant protein labeled at position 446 (B), 448 (C), 449 (D), or 464 (E). Traces represent the pH measured in the external solution; proton uptake was initiated by adding valinomycin (*), and the experiment was terminated by adding CCCP to dissipate the pH gradient (↓). The vertical scale bar represents 6.6×10^{-3} pH unit, and the horizontal bar represents 20 s. The traces were recorded on a chart recorder, digitized on a flat-bed scanner, and processed in Photoshop to remove the background grid and to enhance the visibility of the traces.

across the membrane does the external pH rise, reflecting the Cl^--driven uptake of protons into the vesicles. After the proton flux is allowed to stabilize, the proton ionophore CCCP is added; the sequestered protons are thereby released, and the pH returns to near its starting value. Once transport is activated, though, all of the mutants are able to support Cl^--driven proton uptake that is similar in magnitude and rate when compared with that of the wild-type transporter. These labeled mutants had between 40 and 95% labeling, so if the labeled mutants were not active, we would expect a similar decrease in the measured activity. Our comparisons are not quantitative enough to determine if there are modest changes in the activity of the labeled proteins but do support the conclusion that they are capable of Cl^-/H^+ antiport and that they are therefore useful models for the behavior of the wild-type protein.

pH Dependence of Fluorescence in Labeled Mutants. We initially focused on R helix residues near the interface between the protein interior and the aqueous compartment, reasoning that some of these positions are likely to change their local environment with even subtle conformational changes. Figure 5A shows fluorescence emission spectra from reconstituted, 448C-labeled ClC-ec1 under a series of pH conditions (for reference, Figure 5E shows the R helix, highlighting positions examined here). ClC-ec1 transporters probably are reconstituted in both possible orientations in liposome membranes (*18*). To maximize the symmetry of the system, we include CCCP in the buffer to ensure equilibration of protons across the liposome membrane and to maintain a constant pH inside and outside the vesicles. We are thus looking for changes in the equilibrium populations of states in the transport cycle. For these experiments, we obtain a baseline set of spectra of the proteoliposomes at pH 7.5 (dark blue circles) and then obtain a second set after adding acid to lower the pH to ~4.2 (red triangles), where the protein is near fully activated. Changing the cuvette pH in this way provides an internal reference for every

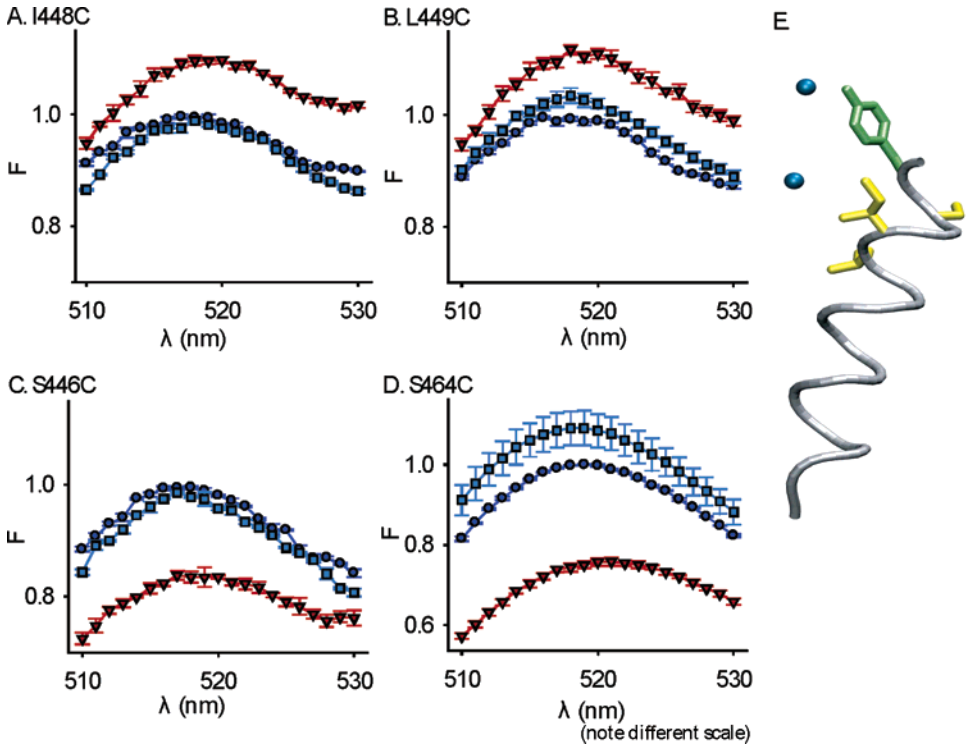

FIGURE 5: Effects of changing pH on ClC-ec1 labeled at R helix positions. Normalized emission spectra are shown for mutant proteins labeled at cysteines introduced at positions 448 (A), 449 (B), 446 (C), and 464 (D). For each position, the initial spectrum at pH 7.5 is colored dark blue (circles), the spectrum after acidification red (triangles), and the spectrum on return to neutral pH light blue (squares). Each experiment was normalized to the maximum emission at the initial neutral pH, and then subsequent experiments were averaged together. $n = 3$ for each mutant except for S464C, for which $n = 2$; error bars indicate the standard error of the mean. A schematic of the R helix is shown (E) for reference. The R helix schematic shows side chains for Y445 (light green), S446, I448, and L449 (yellow). Residue 464 is not resolved in the crystal structure. The two bound chloride ions resolved in the WT structure are shown as blue spheres.

experiment. After measuring the pH, we add base, returning to near the starting pH (light blue squares), to evaluate the reversibility of the spectral changes.

Figure 5A reveals that for labeled 448C there is an increase in the fluorescence emission yield upon acidification, a change which is reversed fully upon return to neutral pH. This result suggests that the fluorophore is reversibly changing its local environment; if its behavior when covalently linked to a protein matches that in free solvent, then it is moving to a more polar locale upon acidification. A similar, but weaker, effect is observed when protein labeled at the adjacent residue, position 449, is examined (Figure 5B). Fluorescence changes still occur when the label is located deeper within the protein. With the mutant labeled at S446C, a residue adjoining the Cl^--coordinating Y445, acidification causes the fluorescence quantum yield to reversibly *decrease* (Figure 5C), suggesting an opposite change in exposure, decreasing the local polarity experienced by the probe.

We also labeled the mutant S464C. This residue, the penultimate position in our construct, is unresolved in the crystal structure (the last resolved residue in Figure 5E is residue 460); we reasoned that it might be distant from any environmental and/or conformational change. Even with this (labeled) mutant, we see a pronounced, but reversible, change in fluorescence emission upon acidification (Figure 5D); as with S446C, the sign of the effect at position 464 suggests that the probe is moving to a more hydrophobic milieu at low pH.

These pH-dependent changes reflect a change in the local "solvent" environment of the fluorophore: what is the physical basis of this effect? A trivial explanation would be that despite its pH independence when free in solution, the inherent electronic properties of the fluorophore are altered when it is attached to the ClC-ec1 protein. We consider this unlikely for several reasons. First, opposite effects of pH on fluorescence at position 446 versus, for example, position 448 suggest that the change in environment depends on the site of labeling. Also, since spectra of Alexa488 reacted with βME or cysteine are similarly pH-independent compared to those of the unreacted fluorophore (data not shown), the fluorescence is independent of the state of the maleimide group. These observations also argue against the fluorophore reporting a change in surface potential on the inner face of the protein at low pH (see below for further evidence). Thus, the fluorescence changes most likely reflect pH-dependent changes in the conformation of the ClC-ec1 protein itself. If the conformational change detected by our methods is related to the mechanism of ion antiport, then it should exhibit a pH dependence similar to that of the activation of transport. To assess this prediction, we examined the pH sensitivity of ClC-ec1 with a label at position 449 in more detail. Titration experiments (Figure 6) demonstrate that the bulk of the fluorescence change for this protein occurs between pH 6.5 and 5, a range similar to that of the activation of Cl^- transport function (*19*). Furthermore, the fluorescence change is saturated above pH 7 and below pH 4 and is fit well by a single-group titration isotherm with an apparent pK_a of ~6.0 (red trace).

Cl^- Concentration Dependence of the Fluorescence Change. We have presented evidence suggesting that ClC-ec1 might undergo a conformational change upon acidification, that the

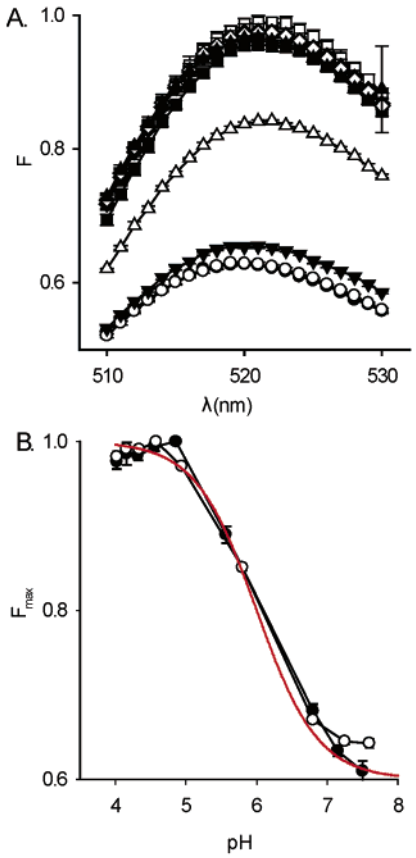

FIGURE 6: pH dependence of fluorescence for labeled L449C. (A) Normalized emission spectra at a series of pH's: 7.6 (●), 7.25 (○), 6.8 (▼), 5.8 (△), 4.94 (■), 4.58 (□), 4.34 (◆), 4.16 (◇), and 4.02 (▲). These data are from a single experiment. Three spectra were taken at each pH value, and the points represent the mean, with error bars indicating the standard error of the mean. After the spectra were obtained, the pH was measured, an aliquot of citric acid added, and the process repeated at the new pH. Points are connected with straight lines. (B) Titration of the fluorescence effect. Data from the wavelength of maximal fluorescence are plotted as a function of pH after correction for added volume. Results from two separate experiments (○ and ●) are superimposed. The experiments are plotted separately because each acid addition resulted in a slightly different pH, particularly near the apparent pK_a. The red trace is a single-site titration isotherm with a pK_a of 6.0.

pH dependence of the change mirrors the pH dependence of activation, and that the fluorescently labeled proteins retain structural and functional integrity. Is this conformational change part of the transport process, or is it an epiphenomenon? We probe for coupling between the conformational change and the transport process by varying the concentrations of the transported anion as well as the proton. To this end, we examined the effects of anions on the fluorescence of labeled mutant ClC-ec1, reasoning that for many transporters different states in the transport cycle have different affinities for their substrate. If this is true for chloride in ClC-ec1, then changing the chloride concentration might change the favored state of the transporter to one with the fluorophore in a different environment.

As noted before, our reconstituted vesicles probably have transporters in both possible orientations. For our pH dependence experiments, we added CCCP to ensure that the proton concentrations are equal inside and outside the vesicles. Equilibrating the Cl^- concentration on both sides of a vesicle would be more difficult since we do not have a

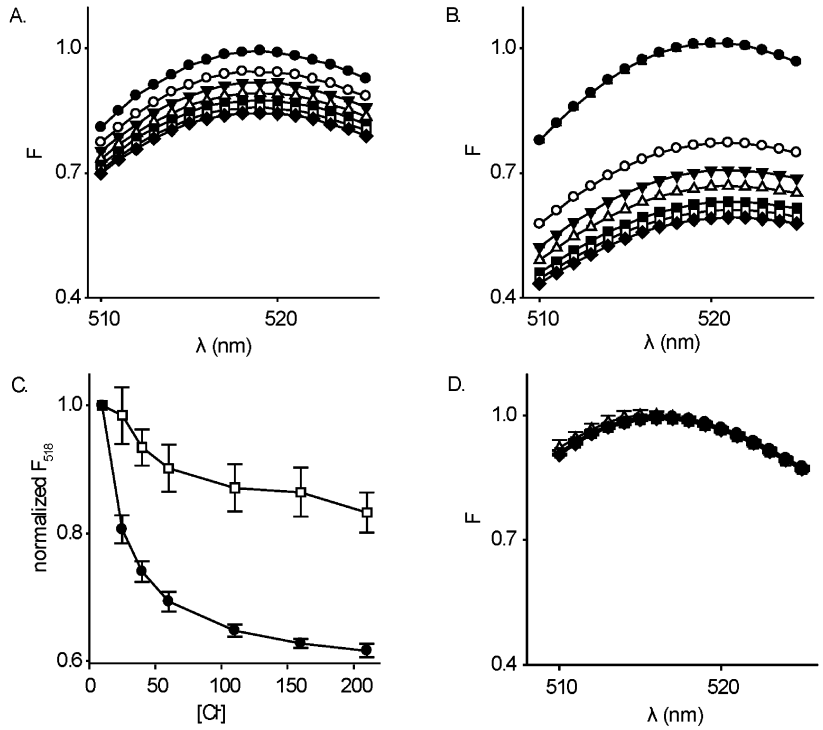

FIGURE 7: Coupling of pH and Cl^- concentration dependence for labeled L449C. Emission spectra are shown at increasing Cl^- concentrations at pH 7.5 (A) and 4.2 (B). The control examining the Cl^- concentration dependence of the free probe at pH 7.5 is shown in panel D. Each panel represents a single experiment. An initial set of spectra were taken at 10 mM Cl^- (●), and then NaCl was added to total concentrations of 25 (○), 40 (▼), 60 (△), 110 (■), 160 (□), and 210 mM (◆). Three spectra were taken at each Cl^- concentration and averaged. Error bars indicate the standard error of the mean. All of the data from each experiment were normalized to the maximum measurement at 10 mM Cl^-. (C) Cl^- concentration dependence of fluorescence at 518 nm. Data from 518 nm in panels A and B were averaged with data from other experiments in which only fluorescence at 518 nm was measured. pH 7.5 data are shown with white circles ($n = 5$) and pH 4.2 data with black circles ($n = 4$). Data are corrected for the volume changes upon addition salt, with a maximum correction of ~6% at 210 mM. Error bars indicate the standard error of the mean. Points are connected with straight lines.

chloride ionophore. Instead, we studied the influence of Cl^- concentration using protein solubilized in detergent micelles. The detergent-solubilized protein runs as a symmetric, sharp peak on gel filtration (data not shown); in addition, pH dependence experiments on fluorescently labeled detergent-solubilized mutants, similar to those in Figure 5, reveal pH-dependent fluorescence changes similar to those we see with reconstituted protein (data not shown). Together, these results suggest that the protein in detergent (DM) remains intact and capable of the conformational change.

To look for coupling between the effects of chloride and protons, we collected emission spectra of ClC-ec1, labeled at position 449, in the presence of varying Cl^- and proton concentrations (Figure 7A,B). Increasing the Cl^- concentration at both pH 4.2 and 7.5 causes a marked decrease in the fluorescence emission of the labeled protein [in comparison, the spectra of the isolated fluorophore are independent of Cl^- concentration in this range (Figure 7D for pH 7.5); data at pH 4.2 are similar but not shown]. Notably, the sensitivity to chloride depends on the pH: the effect of increasing the Cl^- concentration is stronger under acidic conditions than at neutral pH. These differences are highlighted when the normalized peak fluorescence is plotted as a function of Cl^- concentration (Figure 7C). Under acidic conditions, the effect of chloride is saturated near 200 mM. Because we have no measurements in the absence of chloride, it is difficult to determine the apparent dissociation constant for the ion; however, it is clearly less than 50 mM. Although the data at neutral pH have significant scatter, the effects of adding chloride seem to be more evenly distributed over the concentration range that was examined, perhaps suggesting a lower apparent affinity for chloride.

Our observations on the coupling of the fluorescence change to both H^+ and Cl^- concentrations are consistent with the hypothesis that we are observing a conformational change in the protein that is related to the transport process. Another possibility, however, is that both ions affect the surface potential of the protein near the fluorophore, thereby influencing the local electrostatic environment of the probe. To examine this possibility, we compared the magnitude the fluorescence changes caused by adding equal concentrations of different monovalent salts (Figure 8). Since all monovalent anions should have similar effects on screening the surface potential, any differences we observe will therefore reflect differences in specific ion−protein interactions. In this experiment, we measured an initial baseline fluorescence emission at 518 nm in a 10 mM Cl^- buffer; we then added a test salt to a final concentration of 290 mM, for a total of 300 mM monovalent anion, and measured the change in fluorescence. Similar experiments in which the monovalent cation rather than the anion was varied (Li, Na, or K) showed no difference among ions, again supporting the conclusion that the fluorescence changes reflect specific anion−protein interactions. A complication of these experiments is that anions are often effective quenchers of fluorescence; indeed, as shown in Figure 8, free Alexa488 is quenched to varying extents by chloride and bromide (note that we see no quenching up to 200 mM NaCl, as shown in

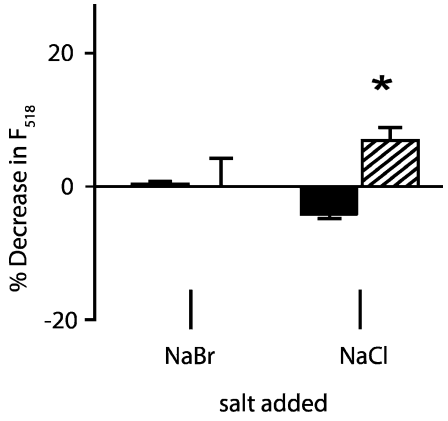

FIGURE 8: Effects of monovalent anions. Baseline fluorescence emission was measured at 518 nm with Alexa488-labeled 449C (black bars) or with free Alexa488 (hatched bars) at 10 mM Cl^-. Either NaCl or NaBr was then added to a total concentration of 290 mM for a total monovalent anion concentration of 300 mM, and a second measurement was taken. The plots represent the percent decrease in the second spectrum (corrected for volume change). Four measurements were made for each salt for the labeled protein and two for the free probe. Differences between the labeled protein and free probe were significant (*) for NaCl ($p = 0.001$). Error bars indicate the standard error of the mean.

Figure 7). However, the effects of these ions on the fluorescence of Alexa488-labeled ClC-ec1 are different than those on the free fluorophore: note that Br^- causes no change in either protein-coupled or free fluorophore, compared with significant shifts in Cl^-. These results imply that the fluorescence changes we observe are, at least in part, due to specific effects on the protein. This difference rules out the possibility that surface potential changes alone cause the fluorescence effects we observe in our experiments. Because the quenching effects dominate those of the individual ions on the protein, these data are not useful in understanding the relative effects of the ions on the conformational change; more directed experiments will be necessary to explore this possibility.

Effects of Mutating the Gating Glutamate. Our data suggest that acidification causes a conformational change in ClC-ec1. What groups must be titrated to trigger this effect? Clearly, glutamate 148 is a prime candidate, since its mutation removes the pH dependence of ClC-ec1 currents (*7*); we therefore labeled constructs carrying both E148A and either I448C or L449C mutations to examine the effects of neutralizing the gating glutamate on fluorescence (E148). We examined the pH dependence of fluorescence for E148A double mutants labeled at position 448 or 449 and reconstituted into proteoliposomes. We observed significant pH dependence with the label at either site (Figure 9). With a probe at residue 448, the fluorescence emission increases at low pH with either glutamate or alanine at position 148, as if the label is moving to a more hydrophilic environment in either case. In contrast, when the adjacent position (449) is labeled, the quantum yield of emission decreases with acidification in the 148A background (compared to an increase for the wild type, E148): the sign of the fluorescence effect therefore depends on the residue at position 148. The persistence of pH-dependent fluorescence at positions 448 and 449 in the E148A mutant suggests that fluorophores at these positions are still sensing a conformational change, but the dramatic effects of the glutamate mutation on the position

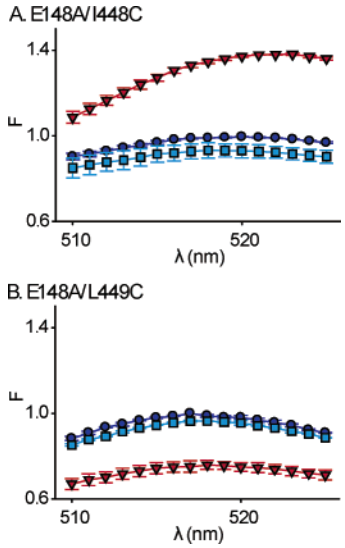

FIGURE 9: Mutations of the gating glutamate. Emission spectra are shown for the Alexa488-labeled double mutants E148A/I448C (A) and E148A/L449C (B). As in Figure 1, initial spectra at pH 7.5 are represented with dark blue circles, pH 4.2 data with red triangles, and data after neutralization with light blue squares. Data from each experiment were normalized to the maximum initial fluorescence (at pH 7.5). $n = 2$ for each double mutant. Error bars indicate the standard error of the mean.

449 mutant reinforce the importance of the gating glutamate. Although glutamate 148 is critically important in determining the response of ClC-ec1 to pH changes, other residues must also contribute to pH sensing.

DISCUSSION

We have developed a system for probing the conformational dynamics underlying transport in a bacterial ClC, ClC-ec1. Here, we demonstrated that we can specifically label R helix residues with an environment-sensitive fluorescent probe and that probes attached at various positions in the helix experience changes in solvent environment upon acid-induced activation of the protein. These fluorescence changes occur in a pH range similar to that of transport activation and depend both on chloride and proton concentrations. Furthermore, the apparent affinity of the chloride-dependent fluorescence change is similar to those recently reported for anion-binding sites in the protein (*20*). These data support the hypothesis that there is a conformational change involving the cytoplasmic side of the protein that occurs as part of its transport cycle. Unexpectedly, these changes apparently extend to include a residue near the carboxy terminus of the protein. Also, fluorescence changes still occur at two positions in the presence of the E148A mutation, despite the decoupling of chloride transport from the proton gradient (and vice versa) in this mutant.

What is the basis of the fluorescence changes? Since the fluorescence of the isolated Alexa488 is pH-independent, the data demonstrate that the fluorescence changes reflect some change in the ClC-ec1 protein itself. What is this change? The simplest explanation is that a conformational change in the protein moves the fluorophore between regions of differing environment upon acidification. Our data suggest that other candidate mechanisms for the fluorescence change are unlikely but do not rule them out. It is possible that changes in the surface electrostatics (caused by pH-dependent

titration of charged group) of the protein could change the excited state of the fluorophore and thereby change its emission properties. However, our observations of salt-dependent fluorescence effects (Figure 8) argue against a surface charge-based electrostatic mechanism. The effects of mutating glutamate 148, fairly distant from the fluorophore, also support the argument that the fluorescence change reflects a conformational change, since this mutation should have a minimal effect on the surface potential of the cytoplasmic side of the protein, yet we see substantial alterations in the fluorescence change between the antiporter containing a wild-type glutamate at position 148 and the E148A mutant.

Fluorescence changes occur with probes at each R helix residue labeled in these experiments. These may reflect a conformational change moving this helix in relation to the rest of the protein; however, other possibilities must also be considered. One alternative is that other parts of the protein, helix D or J, for example, move to shift the exposure of helix R. Nothing in our data precludes this option. Given the relatively long linker (five methylenes) between the maleimide and the fluorophore in Alexa488, we must also contemplate the possibility that acidic conditions expose a binding site for the fluorophore; rather than sensing shifts in solvent access, the fluorescence changes measured would then reflect binding to this site. Common to all of these alternatives is the presence of an underlying conformational change in the protein.

We were surprised to find that the protein labeled at position 464 demonstrated a large fluorescence change upon acidification, since a rather large conformational change would be required to change the solvent exposure of this part of the protein. Without such a negative control, it is difficult to conclusively demonstrate the existence of a conformational change; however, the results discussed above render alternative explanations unlikely.

Several lines of evidence suggest that the acid-induced fluorescence changes we observe likely reflect a conformational change which contributes to the transport process in ClC-ec1. First, the changes occur with a pH dependence (Figure 6) essentially identical to that of transport activation, as reported by Iyer et al. (*19*). Second, the change is sensitive to the chloride concentration (Figure 8) but is inconsistent with a simple surface potential effect. Finally, the chloride dependence and pH dependence are coupled (Figure 7), as expected for a Cl^-/H^+ antiporter.

Given the pH independence of transport in the mutant neutralizing glutamate 148 (*7*), we were initially surprised to find that the neutralization of this residue did not alleviate the pH dependence of the conformational change. Upon further consideration, though, we realized that since ClC-ec1 is indeed a proton transporter, there are probably multiple titratable groups on the pathway taken by H^+ through the protein, a conclusion supported by recent mutagenesis and structural results (*21*). In this light, even though mutation of E148 removes a critical group that mediates a rate-limiting step in transport, other parts of the transport cycle, including other pH-dependent steps, could remain intact. We propose that the pH dependence observed in the E148A mutants results from conformational changes related to these other transport steps.

Detailed inferences regarding the nature of the conformational change are limited by complexities of the transport mechanism. The recent revelation that ClC-ec1 is a H^+/Cl^- antiporter, rather than a Cl^- channel, implies that, when active, the transporter is continually cycling through a series of states at rates in the neighborhood of 10^3 s^{-1} (A. Accardi, personal communication). The fluorescence signal we measure under a given set of conditions therefore represents a weighted average of contributions from multiple conformational states (e.g., external vs internal exposure, bound vs unbound ions). In this light, changes in the fluorescence signal upon activation at low pH reflect changes in the relative occupancies of the various states contributing to the transport cycle resulting, in turn, from changes in the rate-limiting steps in the cycle. Given that measured fluorescence reflects an average of the true fluorescence of multiple conformations, our measurements likely underestimate the maximal change.

What is the magnitude of the ClC-ec1 conformational change? Even though the fluorescence changes we measure are relatively large, it is difficult to infer from these the distances of the underlying movements. At best, fluorescence changes reflect many influences and are not expected to be linear indicators of the position of the fluorophore (*22*). The relatively long linker ($CH_2 \times 5$) connecting the maleimide and the ring system adds further uncertainty to the measurement. On the other hand, we observe changes through the length of the R helix, observations consistent with movements affecting the entire helix. The largest effect we have observed is at position 464. This residue is unresolved in the X-ray crystal structure of ClC-ec1 but seems to be exposed to a more hydrophobic environment (on average) upon acidification.

Our results support the proposition that a conformational change involving the R helix contributes to the transport cycle in ClC-ec1. This implies a complexity in the ClC transport cycle/gating process and is consistent with data implicating an R helix residue in eukaryotic ClC gating (*10*). The hypothesis that a simple side chain movement explains ClC gating was proposed before the diagnosis of dual functional personalities in the ClC family: though such a model could in principle explain channel gating, it is difficult to imagine a mechanism for coupled transport based on such a simple movement. Transporter mechanisms, whether modeled with alternating access (large conformational change) or dual gates (smaller, more localized conformational changes), must limit access of ions from one side of the membrane while simultaneously providing access from the other: coordinated movements on both sides of the binding site are therefore necessary. Experimentally, while the critical role of glutamate 148 in coupled transport is clear (*4*, *5*, *7*), the persistence of pH-dependent fluorescence changes in mutants neutralizing this residue supports the idea of multiple, coordinated movements underlying transport. In eukaryotic ClCs also, the role of the residue corresponding to glutamate 148 in fast gating has been well established; we speculate that the conformational changes reported here could reflect aspects of the slow gating process. Delineating the details of movement in the ClC-ec1 transporter will provide a framework for more detailed explorations of conformational changes associated with gating in eukaryotic ClC channels.

ACKNOWLEDGMENT

Alessio Accardi kindly provided the wild-type ClC-ec1 expression construct. We thank Miguel Holmgren, Merritt Maduke, Kenton Swartz, and Chris Miller for helpful discussions.

REFERENCES

1. Jentsch, T. J., Stein, V., Weinreich, F., and Zdebik, A. A. (2002) Molecular structure and physiological function of chloride channels, *Physiol. Rev. 82*, 503−568.
2. Dutzler, R., Campbell, E. B., Cadene, M., Chait, B. T., and MacKinnon, R. (2002) X-ray structure of a ClC chloride channel at 3.0 Å reveals the molecular basis of anion selectivity, *Nature 415*, 287−294.
3. Jentsch, T. J., Poet, M., Fuhrmann, J. C., and Zdebik, A. A. (2005) Physiological functions of CLC Cl^- channels gleaned from human genetic disease and mouse models, *Annu. Rev. Physiol. 67*, 779−807.
4. Accardi, A., and Miller, C. (2004) Secondary active transport mediated by a prokaryotic homologue of ClC Cl^- channels, *Nature 427*, 803−807.
5. Dutzler, R., Campbell, E. B., and MacKinnon, R. (2003) Gating the selectivity filter in ClC chloride channels, *Science 300*, 108−112.
6. Niemeyer, M. I., Cid, L. P., Zuniga, L., Catalan, M., and Sepulveda, F. V. (2003) A conserved pore-lining glutamate as a voltage- and chloride-dependent gate in the ClC-2 chloride channel, *J. Physiol. 553*, 873−879.
7. Accardi, A., Kolmakova-Partensky, L., Williams, C., and Miller, C. (2004) Ionic currents mediated by a prokaryotic homologue of CLC Cl^- channels, *J. Gen. Physiol. 123*, 109−119.
8. Estevez, R., Schroeder, B. C., Accardi, A., Jentsch, T. J., and Pusch, M. (2003) Conservation of chloride channel structure revealed by an inhibitor binding site in ClC-1, *Neuron 38*, 47−59.
9. Traverso, S., Elia, L., and Pusch, M. (2003) Gating competence of constitutively open CLC-0 mutants revealed by the interaction with a small organic Inhibitor, *J. Gen. Physiol. 122*, 295−306.
10. Accardi, A., and Pusch, M. (2003) Conformational changes in the pore of CLC-0, *J. Gen. Physiol. 122*, 277−293.
11. Lakowicz, J. (1999) *Principles of Fluorescence Spectroscopy*, 2nd ed., Kluwer Academic Publishers, New York.
12. Rajagopalan, P. T., Zhang, Z., McCourt, L., Dwyer, M., Benkovic, S. J., and Hammes, G. G. (2002) Interaction of dihydrofolate reductase with methotrexate: Ensemble and single-molecule kinetics, *Proc. Natl. Acad. Sci. U.S.A. 99*, 13481−13486.
13. Gether, U., Lin, S., and Kobilka, B. K. (1995) Fluorescent labeling of purified β2 adrenergic receptor. Evidence for ligand-specific conformational changes, *J. Biol. Chem. 270*, 28268−28275.
14. Mannuzzu, L. M., Moronne, M. M., and Isacoff, E. Y. (1996) Direct physical measure of conformational rearrangement underlying potassium channel gating, *Science 271*, 213−216.
15. Cha, A., and Bezanilla, F. (1997) Characterizing voltage-dependent conformational changes in the Shaker K^+ channel with fluorescence, *Neuron 19*, 1127−1140.
16. Larsson, H. P., Tzingounis, A. V., Koch, H. P., and Kavanaugh, M. P. (2004) Fluorometric measurements of conformational changes in glutamate transporters, *Proc. Natl. Acad. Sci. U.S.A. 101*, 3951−3956.
17. Maduke, M., Pheasant, D. J., and Miller, C. (1999) High-level expression, functional reconstitution, and quaternary structure of a prokaryotic ClC-type chloride channel, *J. Gen. Physiol. 114*, 713−722.
18. Matulef, K., and Maduke, M. (2005) Side-dependent inhibition of a prokaryotic ClC by DIDS, *Biophys. J.*
19. Iyer, R., Iverson, T. M., Accardi, A., and Miller, C. (2002) A biological role for prokaryotic ClC chloride channels, *Nature 419*, 715−718.
20. Lobet, S., and Dutzler, R. (2006) Ion-binding properties of the ClC chloride selectivity filter, *EMBO J. 25*, 24−33.
21. Accardi, A., Walden, M., Nguitragool, W., Jayaram, H., Williams, C., and Miller, C. (2005) Separate ion pathways in a Cl^-/H^+ exchanger, *J. Gen. Physiol. 126*, 563−570.
22. Kobilka, B. K., and Gether, U. (2002) Use of fluorescence spectroscopy to study conformational changes in the β2-adrenoceptor, *Methods Enzymol. 343*, 170−182.
23. Humphrey, W., Dalke, A., and Schulten, K. (1996) VMD: Visual molecular dynamics, *J. Mol. Graphics 14*, 33−38.
24. Humphrey, W., Dalke, A., and Schulten, K. (1996) VMD: Visual molecular dynamics, *J. Mol. Graphics 14*, 27−38

BI0523815